Rare Metal Materials and Engineering
Volume 52, Issue 8, August 2023
Available online at www.rmme.ac.cn

Science Press

Cite this article as: Zhao Xiaohua, Wang Jincheng, Wang Kaixuan, et al. Numerical Simulation and Experimental Validation on the Effect of Stirring Coils' Parameters on TC17 Ingot During Vacuum Arc Remelting Process[J]. Rare Metal Materials and Engineering, 2023, 52(08): 2676-2682.

ARTICLE

Numerical Simulation and Experimental Validation on the Effect of Stirring Coils' Parameters on TC17 Ingot During Vacuum Arc Remelting Process

Zhao Xiaohua[1,2], Wang Jincheng[1], Wang Kaixuan[2], Fu Jie[2], Xia Yong[2], Lou Meiqi[2], Liu Xianghong[2]

[1] State Key Laboratory of Solidification Processing, Northwestern Polytechnical University, Xi'an 710072, China; [2] Western Superconducting Technologies Co., Ltd, Xi'an 710018, China

Abstract: To reduce the risk of β-flecks, the impact of stirring coils' parameters on ingot composition and grain structure was evaluated in TC17 alloys. A model coupling the temperature, electromagnetic, fluid flow, and the solute field was established using MeltFlow vacuum arc remelting (VAR) software. The results show that Cr concentration at the centre increases gradually from the bottom and then increases sharply within 100 mm to the ingot top, showing unlike tendency compared with locations at the edge and 1/2 diameter of the ingot. The increase in either the stirring coil current or reversal time is beneficial to the decrease in Cr content and the width of equiaxed crystal at the ingot centre, due to the accelerated turbulent velocity, which causes additional mixing within the molten pool. From the macromorphology observations of TC17 ingot, at near half of the lower part of the ingot, the location where the disturbance occurs in the direction of columnar crystal growth is corresponding to the position where Cr content increases, both of which have a relationship with stirring coil parameters. The simulation results fit the experimental data well.

Key words: stirring coils; TC17 titanium alloy; numerical simulation; vacuum arc remelting

Titanium alloys are widely used in aerospace, chemistry, biomedicine, etc, due to their high specific strength, corrosion resistance, and other superior performances[1–3]. Among the large variety of titanium grades, TC17 is a β-rich α-β alloy with excellent strength, toughening, hardenability, and medium-high-temperature properties, making it extensively used in the aeroengine fans and compressor discs[4–5]. With the development of aviation industry in recent years, aviation components with more reliable performance and more homogeneous composition are required. This alloy possesses a relatively large number of alloying elements (Ti5Al2Sn2Zr4 Mo4Cr, 17wt% of all alloying elements), making it difficult to exactly obtain the targeting composition in the manufacturing process[6]. If the melting procedure is not carefully controlled[7], a typical melt-related defect containing a high content of Cr, which has been termed as β-fleck, will frequently occur in TC17 alloy[8]. Experience has shown that once formed, β-flecks are very difficult to eliminate[9]. The defects cause an extremely detrimental influence on the mechanical properties, especially low-cycle fatigue and fracture toughness[10–12], and may impose uncontrollable risks on the service safety of the components[13]. As a consequence, it is of great concern to control the ingot composition, especially the Cr element in TC17 titanium alloy ingot to meet the higher reliability and increasing demand.

Nowadays, industrial TC17 titanium alloys are prepared by the vacuum arc remelting (VAR) techniques, whereby for a better control of the alloy composition during refining, many efforts have been made through studying the affecting factors of ingot chemical distribution and macrostructure. Yin et al[9] studied the formation of β-flecks in Ti-17 alloy by directional solidification experiments, and found that the shape and size of β-flecks arose during the solidification process are determined by the content of enrichment of β-stabilizing elements

Received date: February 11, 2023
Foundation item: Key R&D Project of Shaanxi Province-Industrial Field (2018ZDXM-GY-140)
Corresponding author: Liu Xianghong, Ph. D., Professor, Western Superconducting Technologies Co., Ltd., Xi'an 710018, P. R. China, Tel: 0086-29-86514525, E-mail: xhliu@c-wst.com

and withdrawal rates. Mitchell et al[14] revealed that a critical Rayleigh number can provide a basis for a β-fleck formation criterion if there are appropriate physical data. By calculating the Rayleigh number, the possibility of a downward flow should be estimated. Ng et al[15] reported that appending La_2O_3 nucleant particles to Ti-3Al-8V-6Cr-4Mo-4Zr can promote the columnar-to-equiaxed transition and refine the grain size, thus significantly reducing the β-flecks. At the same time, some researchers also studied the flow in the VAR process. Karimi-Sibaki et al[16] investigated different arc distributions under an axial magnetic field (AMF) in VAR process, and focused on the flow patterns and the resulting melt pool of the Ti-64 ingot. Nikrityuk et al[17] conducted a liquid metal flow driven by a rotating magnetic field of Pb-85wt% Sn alloy under unidirectional solidification. This indicates that there is a relationship between the heat flux and segregation.

It should be noted that electromagnetic stirring is usually employed in the VAR melting practice for titanium alloys. In the VAR process, magnetic stirring is validated with current coils around the mould. This magnetic field interacts with the radial current in the metal to impose a Lorentz force in the angular direction, which in turn causes the molten metal moving in the angular direction. Under this circumstance, the solidification behavior of the VAR metal pool is much more complicated. Yang et al[18] studied the macrosegregation of Fe element during the preparation of Ti-10V-2Fe-3Al alloy in the VAR process and found that the Lorentz force caused by external magnetic field reduces the degree of macrosegregation by stirring the molten pool. Nonetheless, very few studies regarding the effect of parameters of stirring coils, which generates electromagnetic field, on chemical properties and grain structure of industrial TC17 ingot, have been carried out so far. As the traditional experimental techniques do not give access to the remelting and solidification process for the high temperature and lower pressure environment during VAR furnace, the numerical simulation method alternatively can give an insight into the distribution of composition and grain structure[19–21].

To comprehensively explore the influence of stirring coils' parameters on the ingot evolution and consequently the product quality during the VAR process, while seeking suitable process parameters for actual production, simulation and experiments of industrial ingot of TC17 titanium alloy with 720 mm in diameter by triple-melting VAR process were both conducted and mutually verified. Both of the current and reversal times of the stirring coils will be discussed.

1 Materials and Method

1.1 Materials

The material used in the present study was a Ti-5Al-2Sn-2Zr-4Mo-4Cr alloy, also designated as TC17 alloy and its thermophysical properties are presented in Table 1.

It is not easy to obtain physical properties at high temperatures because of the activity of titanium[14]. The temperature-dependent thermal conductivity and dynamic viscosity of this alloy were tested from 23 °C to liquidus temperature (1665 °C) to obtain an accurate boundary condition. Thermal conductivity and dynamic viscosity parameters are shown in Fig. 1. More specifically, compared with the TC17 alloy in the software data-base, the as-received TC17 titanium alloy has lower thermal conductivity and higher dynamic viscosity, especially at higher temperatures. With increasing temperature, the thermal conductivity increases and dynamic viscosity decreases.

1.2 Simulation model

The evolution of the ingot composition and grain structure during the VAR process of TC17 alloy has been simulated while taking into account the coupled thermal, electromagnetic, and flowing evolution phenomena by MeltFlow VAR5.0 software. The model and boundary parameters are summarized in Table 2. It should be noted that

Table 1 Thermal and physical parameters of TC17 alloy

Parameter	Value
Solid density/g·cm^{-3}	4.50
Liquid density/g·cm^{-3}	4.13
Solidus temperature/°C	1608
Liquidus temperature/°C	1665
Coefficient of thermal expansion/×10^{-6} K^{-1}	8.43
Latent heat/×10^{-5} J·kg^{-1}	2.22
Electrical conductivity at 25 °C/×10^{-5} S·m^{-1}	2.33

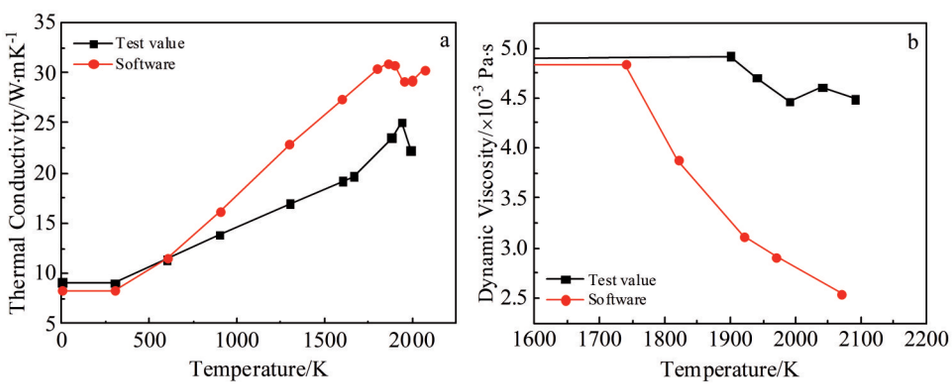

Fig.1 Variation of thermal conductivity (a) and dynamic viscosity (b) with temperature

Table 2 Geometric model and boundary parameters

Parameter	Value
Electrode diameter/mm	640
Ingot diameter/mm	720
Ingot length/mm	2600
Temperature of the inlet cooling water/K	303
Heat loss coefficient of the mould wall/W·m^{-2}	7500
The minimum heat loss coefficient of the gap/W·m^{-2}	400
Heat loss coefficient of the mould bottom/W·m^{-2}	500

in this model the effect of the previous melting on the triple-melting process was considered, so the composition distribution will be more accurate with the actual process.

VAR procedure is performed in a closed furnace chamber under a primary vacuum (Fig. 2). An electric arc is maintained between the tip of the consumable electrode (cathode) and the top of the secondary ingot (anode), which is gradually built up in the mould[22–23]. The ingot solidifies in contact with the mould walls. In addition to the solidified zone, it comprises a mushy zone (part liquid/part solid) and a liquid pool at the top, fed by the liquid metal droplets that are produced at the electrode tip and transferred to the ingot. The arc operates in the direct current mode, with a high current and a low voltage[24]. With power-on stirring coils winding around the mould, the electromagnetic field is created in the molten pool[25]. The current reverses in direction in a regular and rapid manner. This gives rise to an axial magnetic field that reverses in a certain direction (upward and downward). The arc current interacts with the electromagnetic field caused by stirring coils to produce the electromagnetic force, which has an important influence on the molten pool, and ultimately affects composition and macrostructure.

Magnetic stirring caused by stirring coils gives rise to an axial magnetic field, which interacts with the radial current in the metal, causing a Lorentz force in the angular direction.

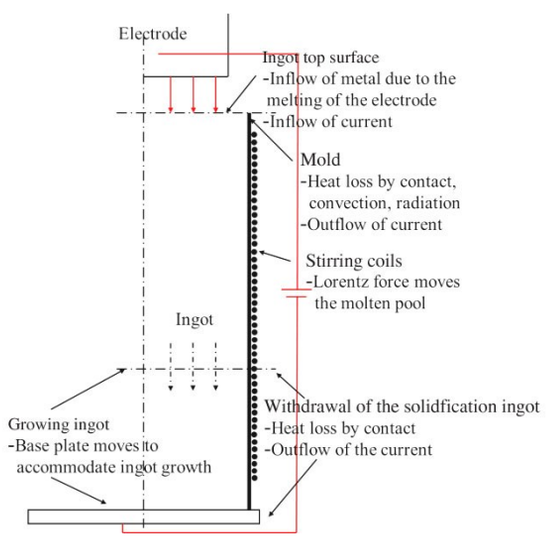

Fig.2 Schematic representation of the VAR process

The equation of Lorentz force in the angular direction is described below.

$$F_\theta = -J_r B_{axial} \quad (1)$$

where F_θ represents Lorentz force in the angular direction, J_r represents the radial current and B_{axial} represents the axial magnetic field. This force creates motion of the liquid metal in the angular direction. Further, the presence of the angular velocity also creates additional mixing or stirring and additional turbulence within the molten pool.

1.3 Schematic design

In order to clarify the effect of stirring coils parameters on the VAR procedure, a comparative study of VAR process is conducted in four cases of 0 A (without stirring coils), 10 A-15 s, 15 A-15 s and 15 A-10 s. The operating conditions are summarized in Table 3, and choose Project II operating conditions to melt for the experiment.

Fig.3 shows the sketch maps of the sampling for the above experiment of TC17 titanium alloy ingots in this work. The cylindrical TC17 titanium alloy ingot was cut along the axial direction in half, giving it a final longitudinal profile. All the chip specimens from the centre, 1/2 diameter (R) and edge of the ingot were drilled equidistantly. After sorting, the composition of the chips was analyzed using inductively coupled plasma based spectrometry method. A longitudinal slab was extracted from the remelted ingot and divided into several parts. Then, each piece was polished and etched in a solution of 20vol% HF, 20vol% HNO_3 and 60vol% H_2O to reveal the solidification structure.

Table 3 Operating conditions at the third-melting

Project	Current/kA	Volts/V	Stirring current/A	Stirring reversal time/s
I	18	28	0	-
II			10	15
III			15	15
IV			15	10

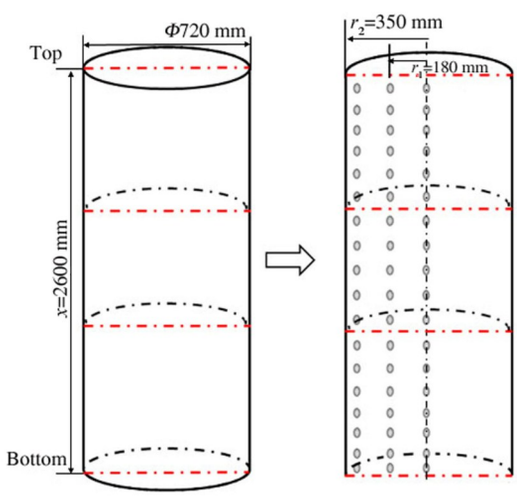

Fig.3 Schematics of ingot sampling

2 Results and Discussion

2.1 Composition of TC17 ingot

Fig.4 shows the Cr elemental distribution profiles from the bottom (distance=0 m) to the top of the ingot which was prepared using the Project II operating parameters along the longitudinal section. The Cr elemental distribution at the centre of the ingot shows a different tendency compared with that at the edge and 1/2*R*. The Cr content is the highest at the centre overall, and the segregation phenomena of Cr fits well with the prediction according to the Ti-Cr binary phase diagrams[26]. The peak value of Cr content at the centre is about 100 mm below the ingot top, mainly due to the fact that it is close to the macro-shrinkage cavity which is formed during hot-topping. The solidification rate decreases during the relative long time hot-topping. When solidification rate is relatively low, solute elements with equilibrium distribution coefficient $k=C_S/C_L<1$, where C_S and C_L are the concentration of an element in the solid and liquid phase, respectively, such as Cr, will concentrate in the liquid/solid front. Thereby, the Cr content sharply increases in the final solidified zone[27]. The experimental value fits well with the simulation value. In conclusion, the prediction model for composition during the VAR process developed in this study is believable.

In order to illustrate the Cr element distribution, Fig. 5 shows the molten pool profiles under different remelting time of Project II melts. It can be seen that during the remelting process, the above 90% liquid zone is defined as red colour at the left side, and the temperature field of the ingot is shown on the right side, which indicates the liquid zone with orange colour and mushy zone with the yellow colour. It is clear that the depth of the molten pool rises with time to a stable stage, in which the depth is about 400 mm, indicating a stable solidification situation, which may be beneficial to the homogeneity of composition. The mushy zone has a similar tendency. When the hot-top begins, the depth of the molten pool decreases.

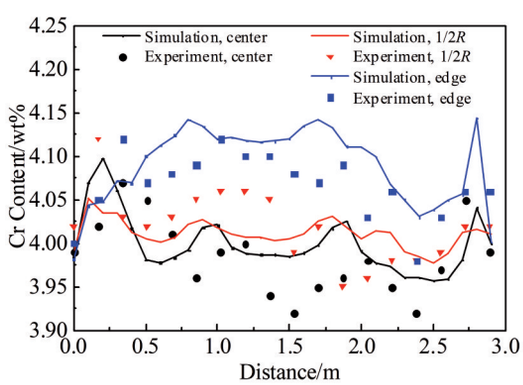

Fig.4 Cr elemental distribution profiles along longitudinal section under Project II operating conditions

As reported by Yuan[27], it is generally agreed that the formation of freckles depends on the factors that contribute to the onset of thermosolutal convection in the mushy zone. Among those factors, the cooling efficiency and the solution flowing in the molten pool are crucial. The cooling effect is better in the part of ingot that thermally contact with the water-cooled copper crucible. In the hot-topping part of the ingot, the temperature gradient is the largest in the near-wall region and the smallest in the centre[28]. When the depth of molten pool changes at the beginning and the end of remelting, the distribution of the Cr element varies. The distribution of the Cr element is relatively stable in the stable-molten-pool-depth stage. It can be seen that the morphology of the molten pool and the mushy zone has a certain effect on the distribution of Cr element.

2.2 Macrostructure of TC17 ingot

The grain structure of the VAR ingot is critically dependent upon the temperature distribution and fluid motion within the molten pool, which in turn are determined by the operational process controlling parameters[29–30]. The macromorphology of TC17 titanium alloys of melt under Project II conditions is shown in Fig.6. As shown, there are three typical zones in the entire cross-section of the ingot. This is the typical macromorphology of VAR ingot, similar to the results reported by Descotes et al[23]. The grain morphology of macrostructure changes in the sequence of equiaxed to columnar grains. At the top of ingots, which is formed in the final solidification, the equiaxed grains usually form at a relatively low solidification rate, accompanied by residual

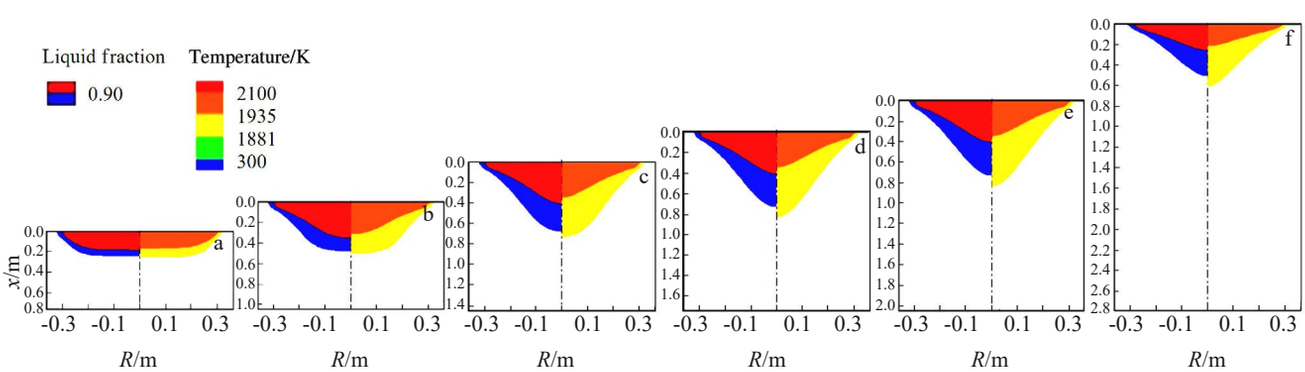

Fig.5 Molten pool profile and temperature map at different moments during the remelting of II melt ingot: (a) 70 min, (b) 140 min, (c) 280 min, (d) 350 min, (e) 420 min, and (f) 700 min

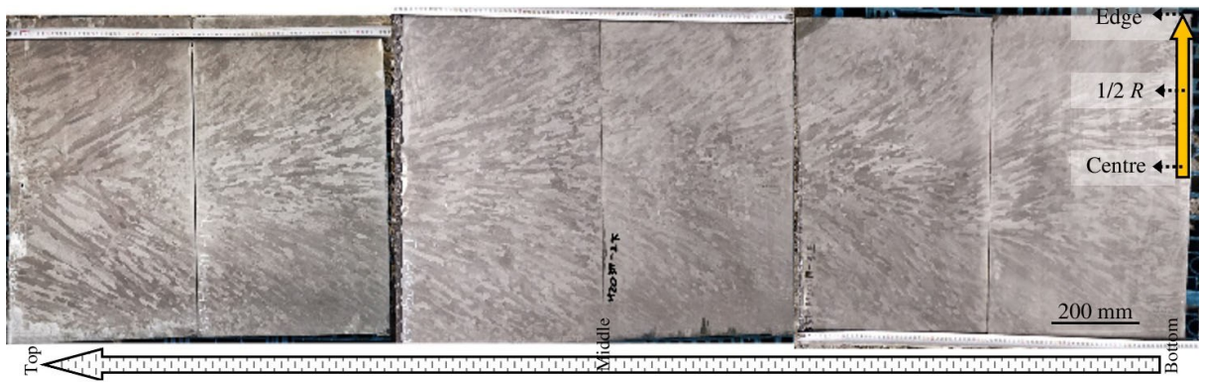

Fig.6 Grain structures of TC17 ingot under Project II condition

liquid and a shallow molten pool. Along the two edges of the ingot, a film of fine equiaxed grains exits. At the bottom of the ingot, there are long and narrow columnar grains perpendicular to the solidification front, with a small angle to the axis. The direction of columnar crystal growth is disturbed at near half height of the lower part of the ingot, which corresponds well to the location where the Cr content rises in Fig. 4. As reported by Yin[9], since the macrostructure is determined by the melting process and solidification conditions, growing dendrite will bring more solute into the interdendritic region and the accumulated solute cannot effectively diffuse into the liquid without additional driving forces[12]. The enrichment of solute will result in the restraining growth of second dendrite arms and channel-like structure forms in the final microstructure.

2.3 Impact of stirring coils' parameters

2.3.1 Composition

In order to illustrate the effect of stirring coils on composition, Fig. 7 shows the Cr content at the ingot centre under four conditions shown in Table 3. It can be found that the distributions of Cr under different stirring parameters are similar. The operating conditions for the maximum fluctuation of Cr is no stirring, and for the minimum it is 15 A-15 s. Cr content distribution is almost the same at 10 A-15 s and 15 A-10 s. It shows that the Cr content reduces as the stirring current and reversal time increase.

As mentioned in Eq.(1), the Lorentz force creates motion of the liquid metal in the angular direction. Further, the angular velocity oscillates with time due to the oscillating force created by the oscillating magnetic field. Thus, the angular velocity affects the radial velocity field due to the presence of the centrifugal force, which causes additional mixing or stirring within the molten pool. Fig. 8 shows the angular velocity clockwise in the entire remelting process. It can be seen that the angular velocity changes periodically and gets smaller. It has a sinusoidal trend in a period, especially at 10 A-15 s. No stirring coils' current indicates no stirring magnetic field, so the angular velocity is 0 in the VAR process. The angular velocity increases as the current increases. The effect of the stirring current is greater than the reversal time, and angular velocity is almost the same at 10 A-15 s and 15 A-10 s, which corresponds to the distribution of Cr elements. It is worth mentioning that in the VAR process, there are complicated flows in the molten pool. Flow disturbances affect temperature gradients and solidification processes, bringing about fluctuations and changes in composition and microstructure, just as the Cr content at 15 A-15 s in Fig. 7. The sharp points may be due to no regular angular velocity in Fig.8.

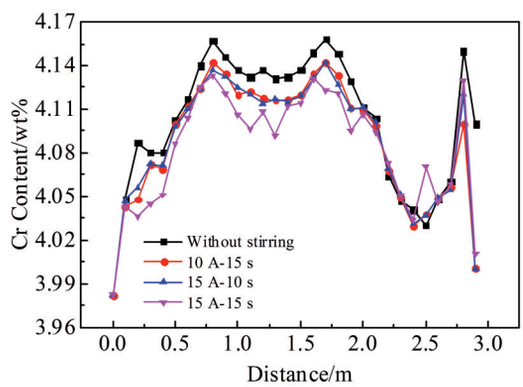

Fig.7 Curves of Cr distribution at centre of ingot under different stirring parameters

2.3.2 Solidification structure

Fig. 9 shows the grain structure of TC17 ingot under the

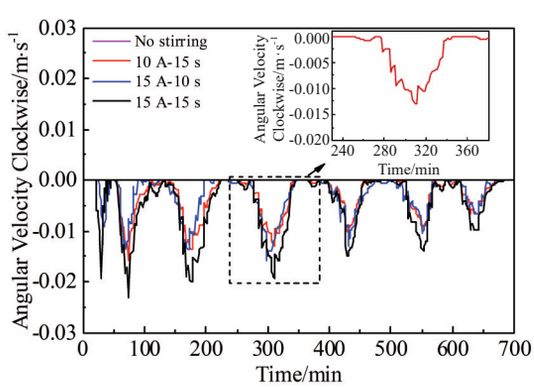

Fig.8 Curves of angular velocity clockwise under different stirring parameters

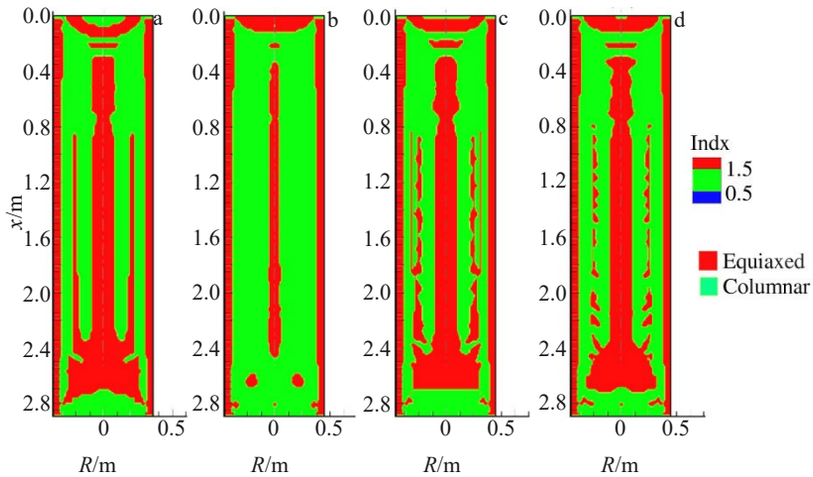

Fig.9 Grain structure of TC17 ingot under different stirring parameters predicted by simulation: (a) without stirring, (b) 10 A-15 s, (c) 15 A-10 s, and (d) 15 A-15 s

four stirring parameters predicted by simulation. It is clearly seen that the common character is that there are three typical grain structures in ingots during the VAR process, including fine equiaxed grains at the ingot edge, equiaxed grains at centre and columnar grains between them. The main difference is the grain morphology at 1/2*R*, especially in the Project II condition. These simulation results are consistent with Kou's results[31].

In the VAR process, the molten metal contacting with the water-cooled copper crucible is cooled fast, resulting in a fast solidification rate and low temperature gradient/solidification rate ratio, thus leading to the formation of a thin layer of fine equiaxed grains at the edge of the ingot[31]. From the above analyses, angular velocity can deepen the molten pool and extends the mushy zone, which decreases the temperature gradient and facilitates nucleation. The lower temperature gradient in the centre of the pool compared to the mid-radius facilitates grain nucleation and results in a central equiaxed structure. From Fig. 8 we can see that the angular velocity is distributed like the sinusoidal trend, suggesting that the equiaxed structure interrupts at 1/2*R* position in 15 A-10 s and 15 A-15 s, but it is stable without stirring. Because of the non-equilibrium at 15 A-10 s and 15 A-15 s, there are disturbing in the molten pool, so the equiaxed structure appears at 1/2*R* position. The stirring flow maintains the balance at 10 A-15 s, so the columnar grains are not interrupted, which fits well with the experiment in Fig. 6. As Davidson[32] reported, the reversal in flow direction can influence the ingot structure.

3 Conclusions

1) A reasonably qualitative agreement can be obtained between the simulation results based on MeltFlow VAR software and experimental results for both Cr content and grain morphology, and precise physical parameters for the TC17 alloys in the experimental results are identified by industrial ingots.

2) Cr elemental distribution at the centre of the ingot, which increases from the bottom followed by a rush at the top, shows unlike tendency compared with locations at the edge and 1/2*R*. There are three typical macromorphologies of VAR ingot. Specifically, at near half of the lower part of the ingot, the position where the disturbance occurs in the direction of columnar crystal growth is corresponding to the position where Cr content rises.

3) The numerical results of the impact of stirring coil parameters indicate that the Cr content reduces as the stirring current and reversal time increase, because the angular velocity causes additional mixing or stirring within the molten pool. Finally, the grain structure may also be affected by the stirring coils.

References

1 Zhang R, Yu Q, Ritchie R O *et al. Science*[J], 2021, 373: 1363
2 Zou C X, Li J S, Wang W Y *et al. Acta Materials*[J], 2021, 202: 211
3 Zhu Y, Zhang K, Meng Z *et al. Nature Materials*[J], 2022, 21: 1258
4 Yang Y, Zhang H, Qiao H C. *Journal of Alloys and Compounds*[J], 2017, 722: 509
5 Huang B, Miao X F, Luo X. *Materials Characterization*[J], 2019, 151: 151
6 Lütjering G, Williams J C. *Titanium*[M]. Berlin: Springer, 2007
7 Bomberger H B, Froes F H. *JOM*[J], 1984, 36: 39
8 Ng C H, Bermingham M J, Dargusch M S. *Additive Manufacturing*[J], 2021, 39: 101 855
9 Yin X C, Liu J R, Wang Q J *et al. Journal of Materials Science & Technology*[J], 2020, 48: 36
10 Shamblen C E. *Metallurgical and Materials Transactions B*[J], 1997, 28(5): 899
11 Zeng W D, Zhou Y G. *Materials Science and Engineering*[J], 1999, 260: 203
12 Zeng W D, Zhou Y G, Yu H Q. *Journal of Materials*

Engineering and Performance[J], 2000, 9(2): 222
13 Cai J M, Cao C X. *Hangkong Fadongji Taiheji Cailiao Yu Yingyong Jishu*[M]. Beijing: Metallurgical Industry Press, 2021 (in Chinese)
14 Mitchell A, Kawakami A, Cockcroft S L. *High Temperature Material Process*[J], 2006, 25: 337
15 Ng C H, Bermingham M J, Yuan L. *Acta Materialia*[J], 2022, 224: 117 511
16 Karimi-Sibaki E, Kharicha A, Vakhrushev A. *Journal of Materials Research and Technology*[J], 2022(19): 183
17 Nikrityuk P A, Eckert K. *International Journal of Heat and Mass Transfer*[J], 2006, 49: 1501
18 Yang Z J, Kou H C, Li J S *et al. Journal of Materials Engineering and Performance*[J], 2010, 20: 65
19 Kondrashov E N, Musatov M I, Maksimov A Yu. *Journal of Engineering Thermophysics*[J], 2007, 1(16): 19
20 Delzanta P O, Chapellea P, Jardy A. *Journal of Materials Processing Technology*[J], 2019, 266: 10
21 Cui J J, Li B K, Liu Z Q. *Journal of Materials Research and Technology*[J], 2022, 20: 1912
22 Mir H E, Jardy A, Bellot J P. J*ournal of Materials Processing Technology*[J], 2021, 210: 564
23 Descotes V, Quatravaux T, Bellot J P *et al. Metals*[J], 2020, 10(4): 541
24 Woodside C R, King P E, Nordlund C. *Metallurgical and Materials Transactions B*[J], 2013, 44: 154
25 Kou H C, Zhang Y J, Yang Z J *et al. International Journal of Engineering & Technology*[J], 2014, 12: 50
26 Massalski T B, Murray J, Bennett L. *American Society for Metals*[J], 1986, 2: 1118
27 Yuan L, Lee P D. *Acta Materialia*[J], 2012, 60(12): 4917
28 Cui J J, Li B K, Liu Z Q. *Journal of Materials Research and Technology*[J], 2022, 18: 3991
29 Kermanpur A, Evans D G, Siddall R J. *Journal of Materials Science*[J], 2004, 39: 7175
30 Xu X, Zhang W, Lee P D. *Metallurgical and Materials Transactions A*[J], 2022, 33: 1805
31 Kou H C, Zhang Y J, Li P F *et al. Rare Metal Materials and Engineering*[J], 2014, 43(7): 1537
32 Davidson P A, He X, Lowe A J. *Materials Science and Technology*[J], 2000, 16: 13

真空自耗电弧熔炼过程中搅拌线圈参数对TC17铸锭成分和组织影响的数值模拟与实验验证

赵小花[1,2]，王锦程[1]，王凯旋[2]，付　杰[2]，夏　勇[2]，楼美琪[2]，刘向宏[2]
(1. 西北工业大学 凝固技术国家重点实验室，陕西 西安 710072)
(2. 西部超导材料科技股份有限公司，陕西 西安 710018)

摘　要：采用MeltFlow VAR软件建立了真空自耗电弧熔炼（VAR）过程中温度、电磁、流动和溶质场的耦合模型，通过数值模拟与实验验证的方法研究了搅拌电流和周期对TC17钛合金铸锭成分和组织的影响规律。结果表明，铸锭中心的Cr元素浓度从底部逐渐升高，在铸锭头部100 mm范围内出现激增，与铸锭边缘和1/2半径处表现出不同的趋势。施加搅拌磁场，有利于铸锭心部Cr元素的降低和1/2直径处等轴晶区域宽度的减小。增加搅拌线圈电流或延长搅拌磁场的周期，可以降低铸锭心部Cr元素含量并减小1/2直径处等轴晶区域宽度。这主要是因为搅拌磁场引起的角速度，加剧了熔池内湍流的速度。采用工程化规格的TC17铸锭实物解剖可知，铸锭下部柱状晶生长方向发生扰动的位置与Cr含量上升的位置相对应，均与该位置搅拌磁场的作用相关。数值模拟结果与实验数据吻合较好。

关键词：搅拌线圈；TC17钛合金；数值模拟；真空自耗电弧熔炼

作者简介：赵小花，女，1985年生，硕士，高级工程师，西部超导材料科技股份有限公司，陕西 西安 710018，电话：029-86514525，E-mail：him-1956_110@163.com